Supplement of Atmos. Chem. Phys., 20, 7291–7306, 2020
https://doi.org/10.5194/acp-20-7291-2020-supplement

Atmospheric Chemistry and Physics
Open Access
EGU

Supplement of

Impacts of water partitioning and polarity of organic compounds on secondary organic aerosol over eastern China

Jingyi Li et al.

Correspondence to: Qi Ying (qying@civil.tamu.edu) and Jianlin Hu (jianlinhu@nuist.edu.cn)

Supplementary Material

The CMAQ model treats high and low NO_x SOA formation pathways during OH oxidation by allowing the lumped RO_2 radical to competitively react with HO_2 and NO. Using the lumped ARO1 species as an example, an SOA formation specific RO_2 radical ARO1RO2 is added as a gas phase reaction product with OH:

$$\text{ARO1} + \text{OH} \rightarrow \text{ARO1RO2} + \text{products}$$

The ARO1RO2 can react with both HO_2 and NO, as shown in the following two reactions:

$$\text{ARO1RO2} + \text{HO}_2 \rightarrow \text{HO}_2 + \text{TOLNRXN}; \quad k_1$$

$$\text{ARO1RO2} + \text{NO} \rightarrow \text{NO} + \text{TOLHRXN}; \quad k_2$$

Details of the determination of the rate constants can be found in Carlton et a. (2010). The TOLNRXN and TOLHRXN are counter species that track how much ARO1 is reacted through low NO_x and high NO_x pathways, respectively, in one gas chemistry time step. The concentrations of these counter species are passed into the aerosol module to calculate the formation semi-volatile products (TOL1 and TOL2) in the high NO_x pathway and non-volatile products (TOL3) in the low NO_x pathway, using the mass-specific yields, as listed in Table S1 and S2. Equilibrium partitioning of TOL1 and TOL2 in the gas phase and their counterparts ATOL1 and ATOL2 in the organic phase are affected by temperature and the amount of absorbing organics in the aerosol phase. Similar treatments are applied to the other lumped aromatic compounds ARO2, with xylene as a representative and most abundant species in that group, and to benzene. SOA formation from lumped long-chain alkene species ALK5, and isoprene and monoterpenes are not considered as NO_x dependent and are represented by equilibrium partitioning of one or two semi-volatile oxidation products. Details of the mass-specific yields of semi-volatile products and other related parameters can be found in Table S1 and S2.

Table S1. Properties of SV-SOA used in the model following Pankow et al. (2015).

Species	Precursor	Production Pathways	Molecular Weight ($g\ mol^{-1}$)	OM:OC	α^a ($g\ g^{-1}$)	SVP[b] (298K, atm)
ALK	Alkene	OH	180	2.14	0.0865	2.72E-12
BNZ1	Benzene	OH high-NO_x	161	2.68	0.0900	4.58E-11
BNZ2	Benzene	OH high NO_x	134	2.23	1.1100	2.03E-08
TOL1	Toluene	OH high NO_x	163	2.26	0.2545	3.49E-10
TOL2	Toluene	OH high NO_x	175	1.82	0.7623	2.97E-09
XYL1	Xylene	OH high NO_x	174	2.42	0.2545	1.85E-10
XYL2	Xylene	OH high NO_x	185	1.93	0.7623	4.55E-09
ISO1	Isoprene	OH	132	2.20	0.5104	2.15E-08
ISO2	Isoprene	OH	133	2.23	0.0634	1.13E-10
TRP1	Monoterpenes	OH/O_3/NO_3	177	1.84	0.1811	1.03E-09
TRP2	Monoterpenes	OH/O_3/NO_3	198	1.83	0.5905	1.37E-08
SQT	Sesquiterpenes	OH/O_3/NO_3	273	1.52	1.5370	1.09E-09

[a]mass-based stoichiometric yield from parent hydrocarbon reaction
[b]SVP is saturation vapor pressure

Table S2. Properties of NV-SOA used in the model following Pankow et al. (2015).

Species	Precursor	Production Pathways	Molecular Weight	OM:OC	α[a] ($g\ g^{-1}$)	SVP[b] (298K, atm)
BNZ3	Benzene	OH low NO_x	180	3.0	0.666	1.43E-14
TOL3	Toluene	OH low NO_x	194	2.7	0.570	5.39E-15
XYL3	Xylene	OH low NO_x	218	2.3	0.612	1.18E-13
AIEPOX	Isoprene	Acid-catalyzed	211	2.2	NA[c]	2.32E-15
AIMAE	Isoprene	Acid-catalyzed	211	2.2	NA	2.32E-15
AGLY AMGLY	BVOCs and aromatics	Heterogeneous uptake	211	2.2	NA	2.32E-15
AOLGA	Anthropogenic VOCs	Oligomerization	206	2.5	NA	1.43E-14
AOLGB	Biogenic VOCs	Oligomerization	248	2.1	NA	7.58E-16

[a]mass-based stoichiometric yield from parent hydrocarbon reaction

[b]SVP is saturation vapor pressure

[c]NA indicates not applicable

Table S3. Properties of POA used in the model.

POA	Molecular weight	Molar Fraction to POA
tetracosanoic acid	368	0.01
acetonyl syringol	185	0.01
C29 n-alkane	408	0.08
phthalic acid	166	0.1
benzo(ghi)-perylene	276	0.1
2,6-naphthalene-diacid	216	0.1
butanedioic acid	118	0.1
octadecanoic acid	284	0.1
17.alpha.(H)-21.beta.(H)-hopan	412	0.1
unknown compounds	390	0.3

Table S4. Monthly total emissions of major SOA and POA precursors during January and July of 2013 of the whole domain (Tg).

Species	January	July
Gaseous		
Alkanes	0.26	0.24
Aromatics	0.42	0.43
Isoprene	5.6E-2	2.5
Monoterpenes	6.3E-2	0.65
Sesquiterpenes	1.8E-3	5.4E-2
Particulate		
POA	0.80	0.29

Table S5 List of cities with meteorology observations in different regions.

Region	City
Northeast China (Northeast)	Heihe, Qiqihaer, Xinganmeng, Suihua, Yichun, Jiamusi, Shuangyashan, Songyuan, Haerbin, Jixi, Mudanjiang, Siping, Changchun, Yanbian, Fuxin, Fushun, Jilin, Chaoyang, Jinzhou, Shenyang, Benxi, Chunggang, Tonghua, Baishan, Yingkou, Dandong, Dalian
North China Plain (NCP)	Hulunbe'er, Xilinguole, Alashanmeng, Baotou, Bayanzhuoer, Wulanchabu, Huhehaote, E'erduosi, Zhangjiakou, Shijiazhuang, Xingtai, Tongliao, Chifeng, Chengde, Zhangjiakou, Qinhuangdao, Beijing, Tianjin, Tangshan, Baoding, Cangzhou, Dezhou, Binzhou, Yantai, Weihai, Liaocheng, Jinan, Tai'an, Zibo, Weifang, Qingdao, Heze, Jining, Linxi, Rizhao
Northwest China (Northwest)	Hami, Jiuquan, Lanzhou, Haixi, Zhangye, Wuwei, Haibei, Xining, Hainan*, Dingxi, Yingchuan, Yulin, Zhongwei, Wuzhong, Yan'an, Pingliang, Qingyang, Yushu, Guoluo, Gannan, Longnan, Tianshui, Baoji, Xianyang, Weinan, Hanzhong, Xi'an, Ankang
Yangtze River Delta (YRD)	Xuzhou, Lianyungang, Huai'an, Yancheng, Nanjing, Ningbo, Nantong, Shanghai, Changzhou, Hangzhou, Zhoushan, Shaoxing, Quzhou, Lishui, Taizhou, Wenzhou
Central China (Central)	Datong, Xinzhou, Lvliang, Taiyuan, Jinzhong, Anyang, Yuncheng, Jincheng, Huangnan, Sanmenxia, Luoyang, Zhengzhou, Nanyang, Zhoukou, Shiyan, Xiangyang, Zhumadian, Xinyang, Jingmen, Huanggang, Enshi, Yichang, Wuhan, Zhangjiajie, Yueyang, Jiujiang, Huaihua, Changde, Changsha, Shaoyang, Hengyang, Yichun, Ji'an, Zhengzhou, Hanzhong, Nanyang, Zhoukou, Shiyan, Xiangyang, Zhumadian, Xinyang, Jingzhou, Yongzhou, Chenzhou, Ganzhou, Haozhou, Fuyang, Xinyang, Bengbu, Liuan, Hefei, Wuhu, Anqing, Huangshan, Jiujiang, Jingdezhen, Nanchang, Fuzhou, Luoyang
Sichuan Basin (SCB)	Aba, Ganzi, Chengdu, Mianyang, Ya'an, Leshan, Yibin, Liangshan, Dazhou, Nanchong, Chongqing, Neijiang, Luzhou, Mianyang
Pearl River Delta (PRD)	Sanya, Qingyuan, Shaoguan, Heyuan, Meizhou, Zhaoqing, Guangzhou, Maoming, Shenzhen, Shanwei, Qinzhou, Zhanjiang, Yangjiang, Jiangmen, Haikou, Dongfang, Danzhou, Qionghai, Sansha
Southwest China (Southwest)	Bijie, Tongren, Guiyang, Qiandongnan, Qianxinan, Qiannanbu, Qiandongnan, Guilin, Nanping, Hechi, Liuzhou, Wuzhou, Baise, Guigang, Congzuo, Nanning, Beihai

*Hainan Tibetan Autonomous Prefecture

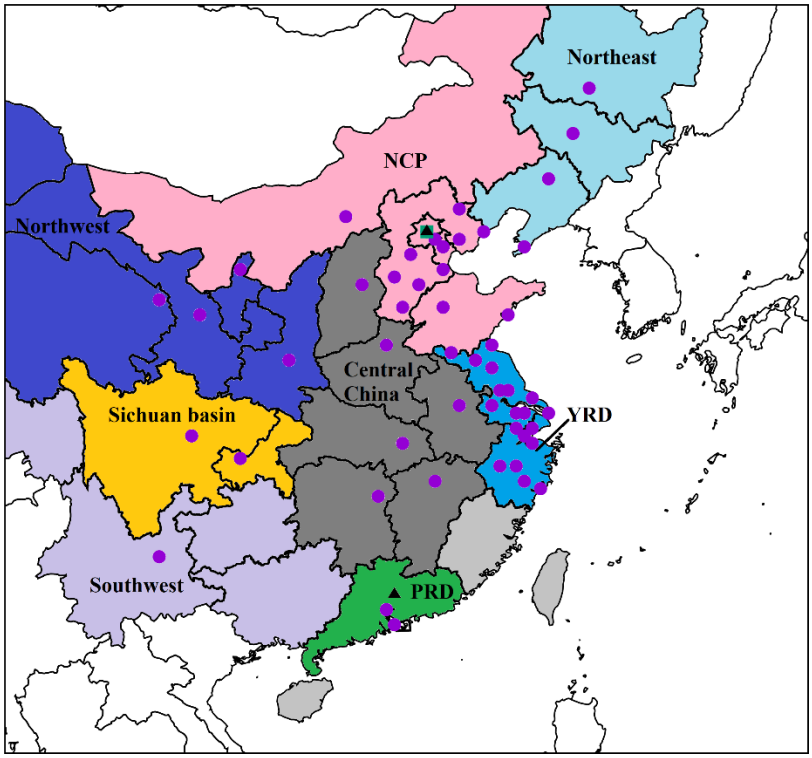

Figure S1. The domain of this study and locations of monitoring sites of $PM_{2.5}$ (dot), OC (triangle) and OA (rectangle). The figure also shows geographical areas in different colors. NCP represents the North China Plain, YRD represents the Yangtze River Delta, and PRD represents the Pearl River Delta.

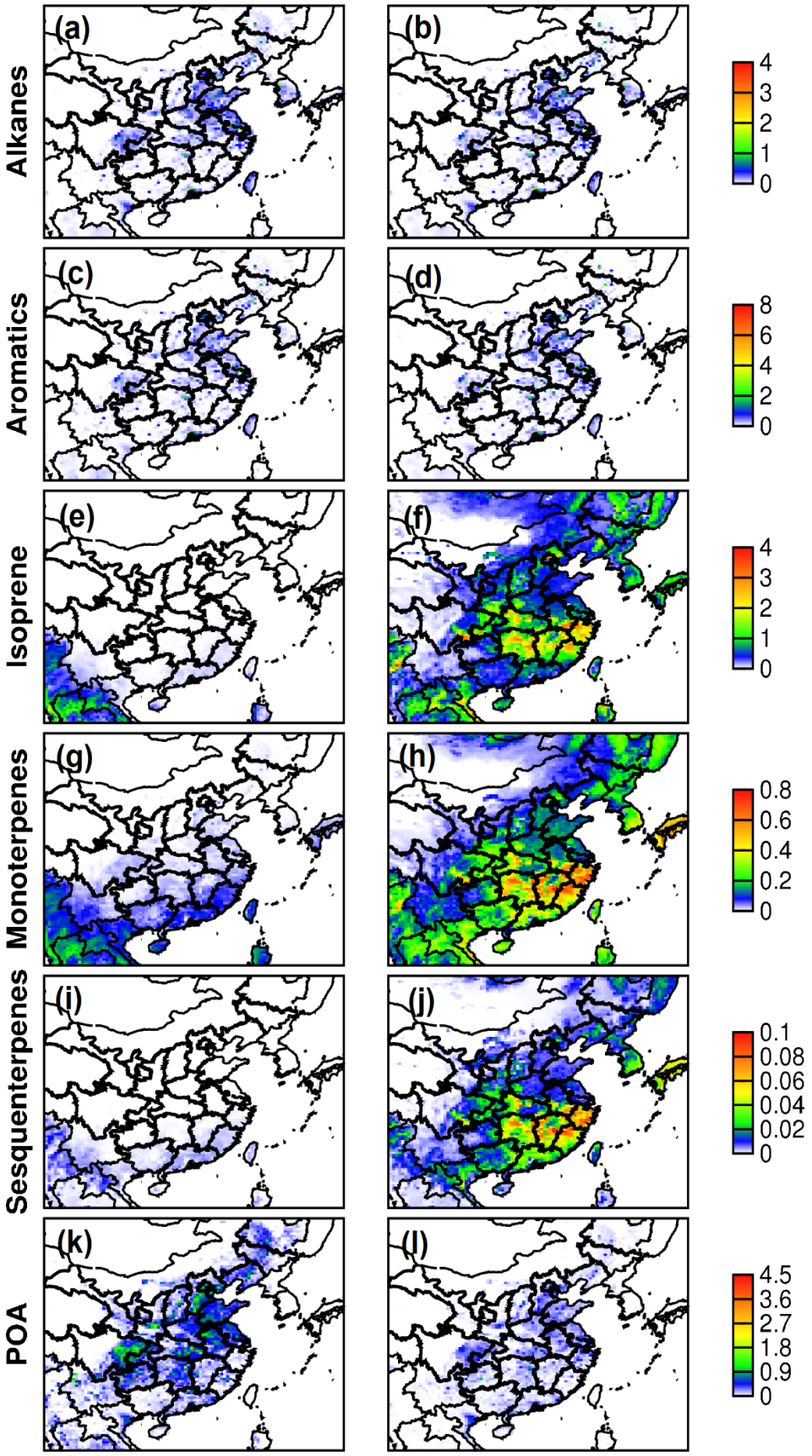

Figure S2. Monthly total emissions of major SOA and POA precursors over the domain during January (left column) and July (right column), 2013. Units are Gg.

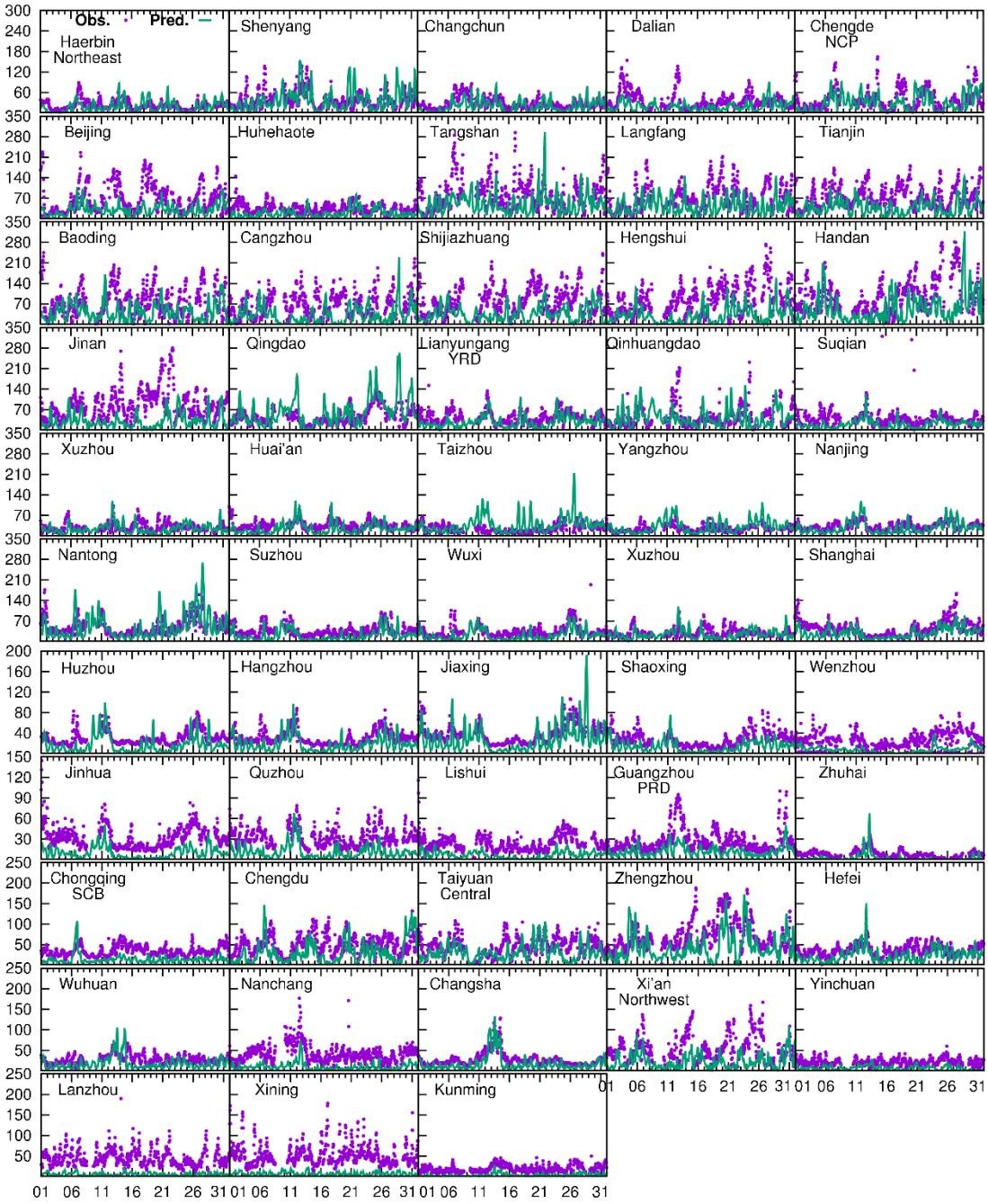

Figure S3. Comparison of observed (dots) and predicted (lines) $PM_{2.5}$ concentration ($\mu g\ m^{-3}$) at monitoring sites shown in Figure S1 during July of 2013.

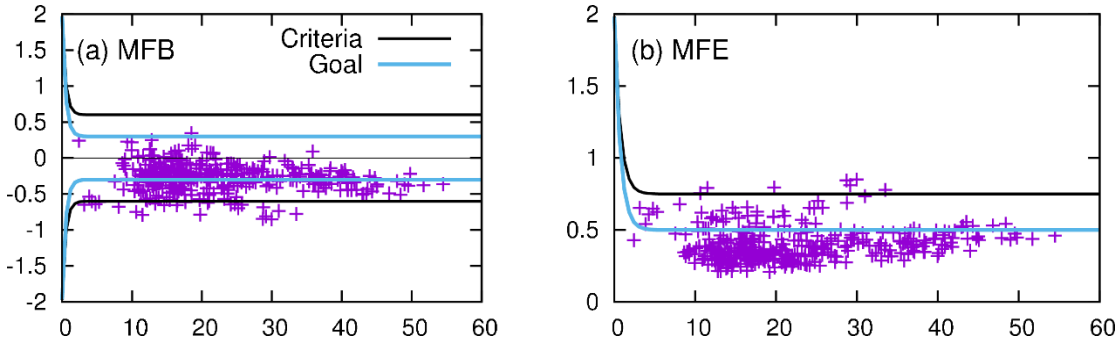

Figure S4. Statistical analysis of modeled $PM_{2.5}$ in July of 2013 at monitoring sites shown in Figure S1.

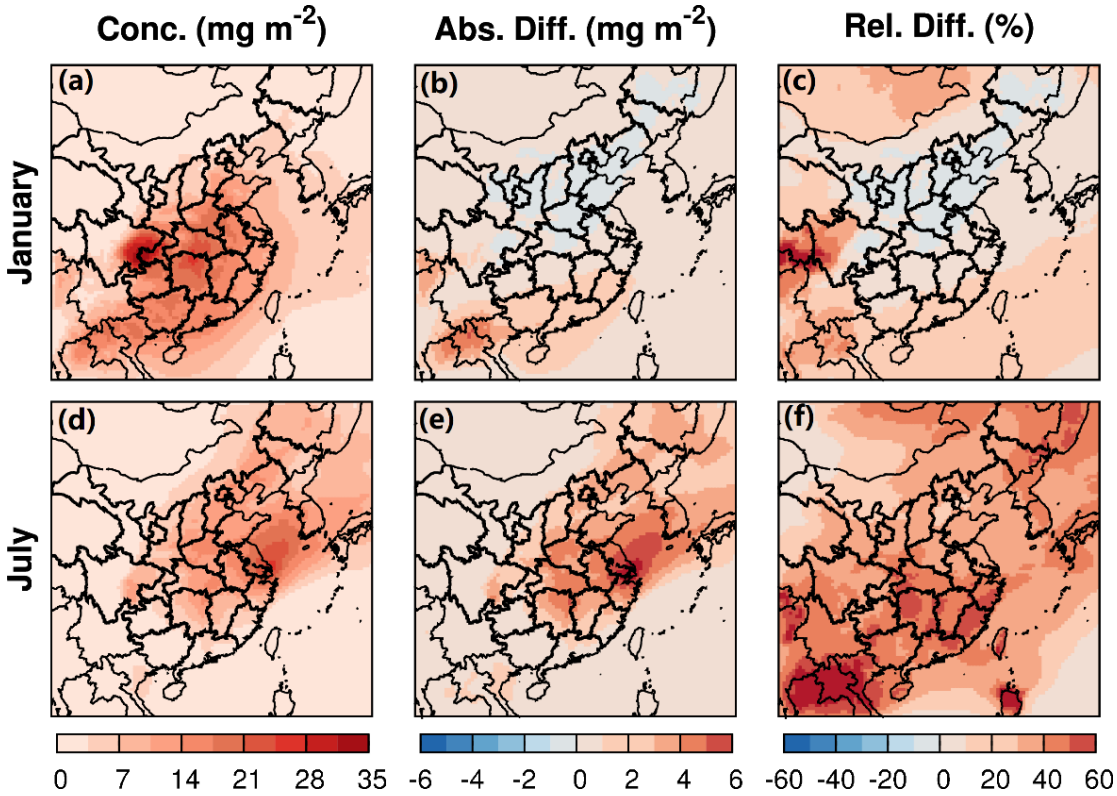

Figure S5. Monthly averaged SOA column concentration from C3 and absolute and relative changes due to water partitioning into OPM and nonideality of the organic–water mixture during January (top) and July (bottom). "Abs. Diff." represents absolute differences (C3-BC); "Rel. Diff." represents relative differences ((C3-BC)/BC; %).

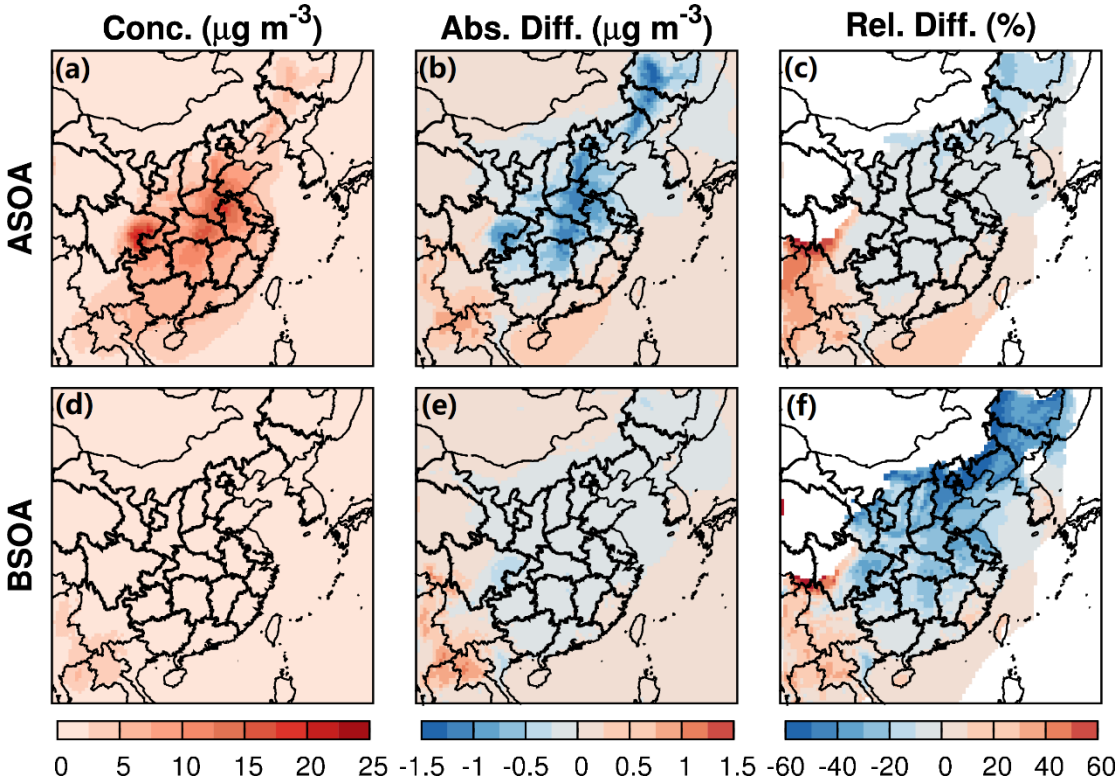

Figure S6. Monthly averaged surface anthropogenic SOA (ASOA) and biogenic SOA (BSOA) from C3 and absolute and relative changes due to water partitioning into OPM and nonideality of the organic–water mixture during January of 2013. "Abs. Diff." represents absolute differences (C3-BC); "Rel. Diff." represents relative differences ((C3-BC)/BC; %). Relative differences are shown in areas with monthly averaged SOA concentrations greater than 1 μg m^{-3}.

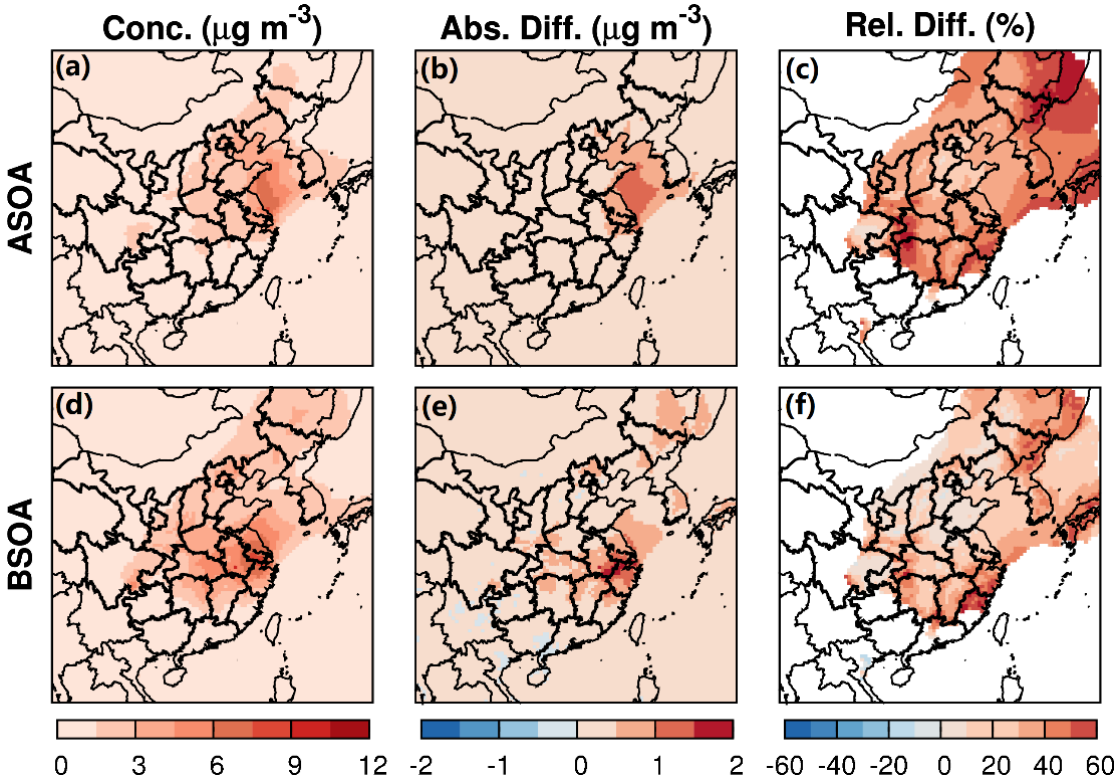

Figure S7. Same as Figure S6 but for July of 2013.

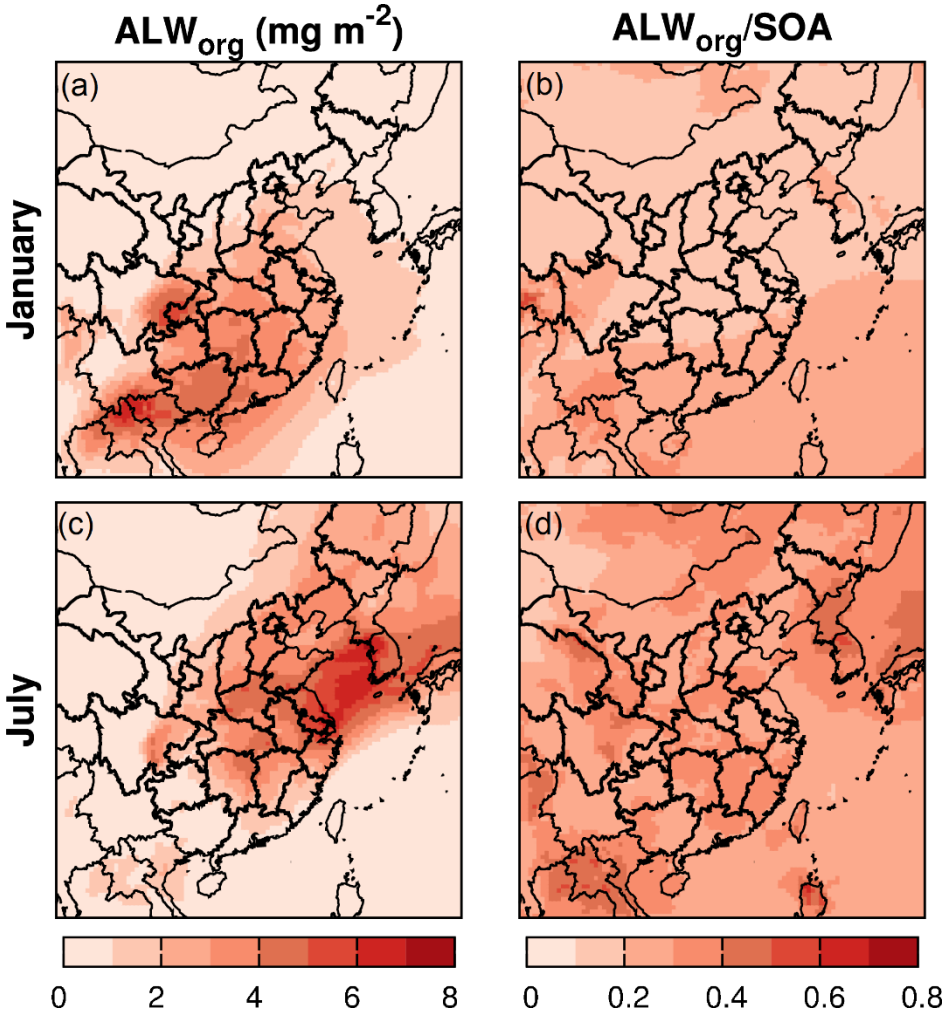

Figure S8. Monthly averaged column concentration of ALW_{org} and the ratio to SOA column concentration in January and July of 2013.

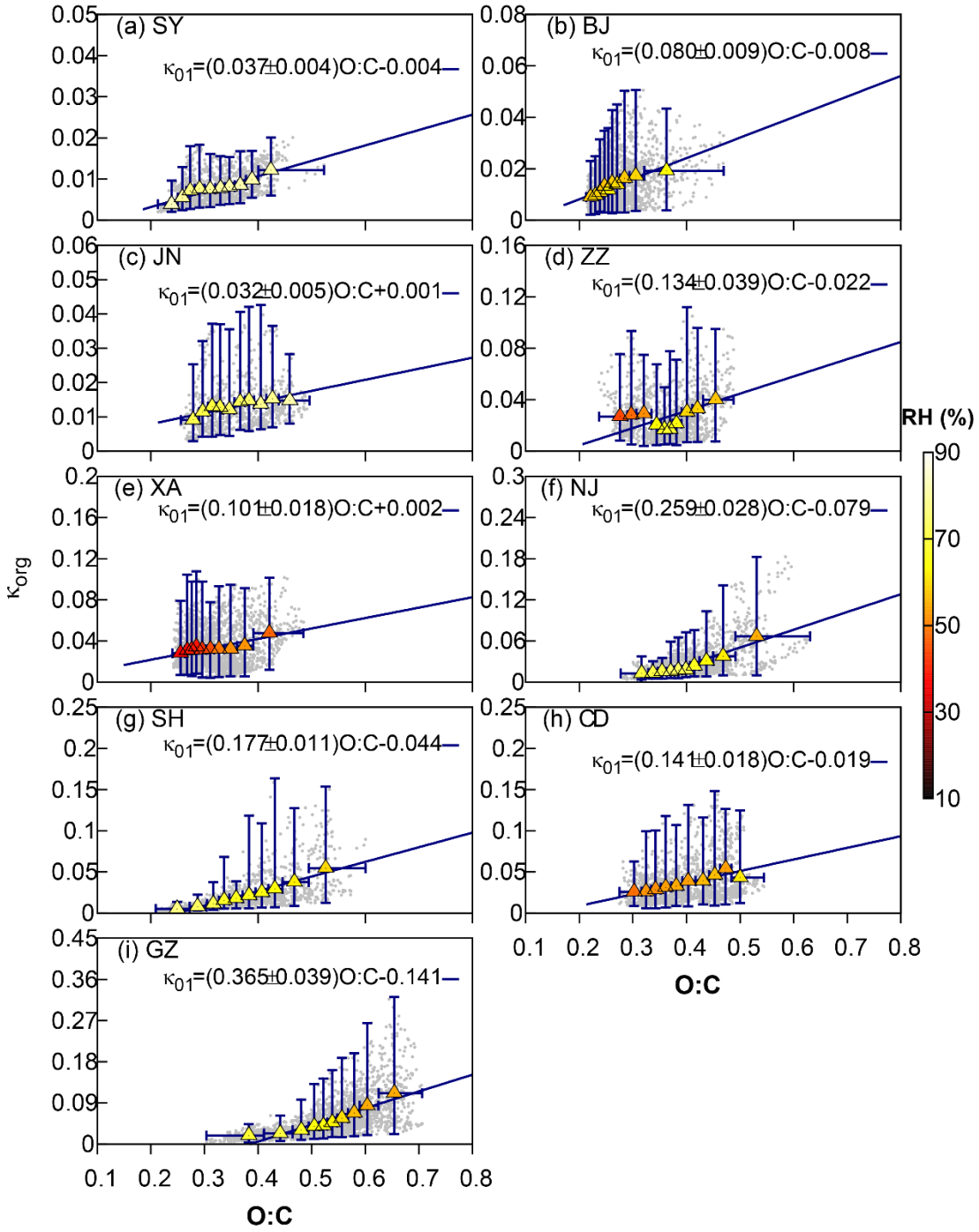

Figure S9. The correlation of hygroscopicity of OA (κ_{org}) and O:C in nine representative cities including Shenyang (SS), Beijing (BJ), Jinan (JN), Zhengzhou (ZZ), Xi'an (XA), Nanjing (NJ), Shanghai (SH), Chengdu (CD), and Guangzhou (GZ) in January of 2013. O:C ratios are categorized into ten bins. In each bin, the ranges of O:C and κ_{org} are represented by bars. The mean values of O:C and κ_{org} are represented by triangles colored by the averaged RH of each bin. The correlation of κ_{org} and O:C is fitted with reduced major–axis regression.

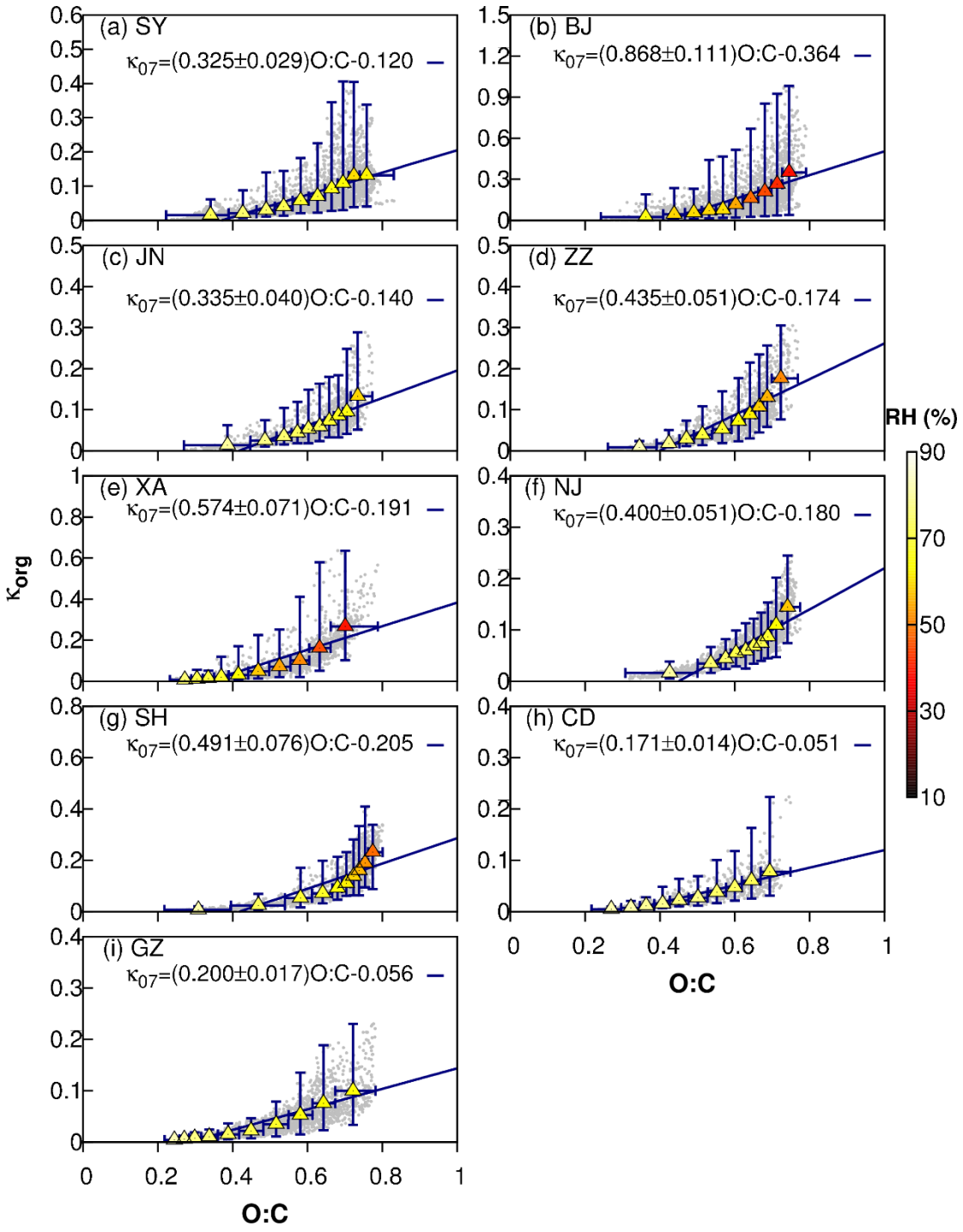

Figure S10. Same as Figure S9 but for July of 2013.

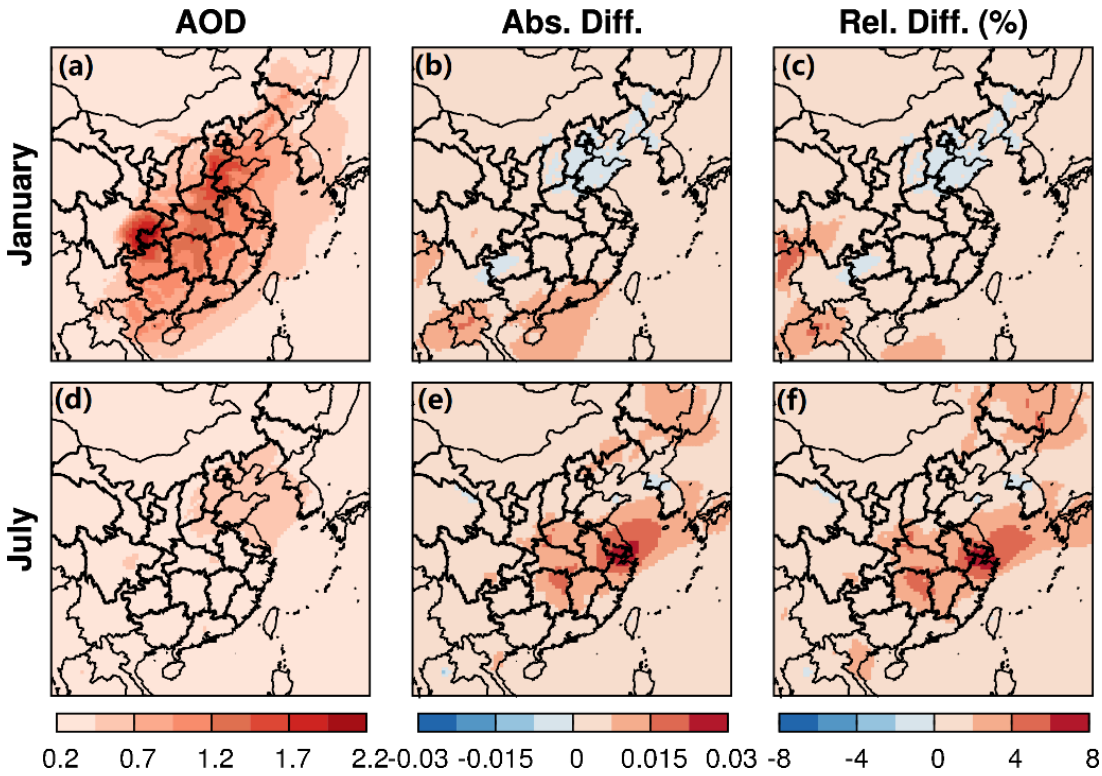

Figure S11. Monthly averaged AOD at 550nm calculated with fine aerosol extinction coefficient by Mie theory and the monthly averaged daily maximum impacts due to water partitioning and non-ideality of the organics–water mixture during January and July of 2013.

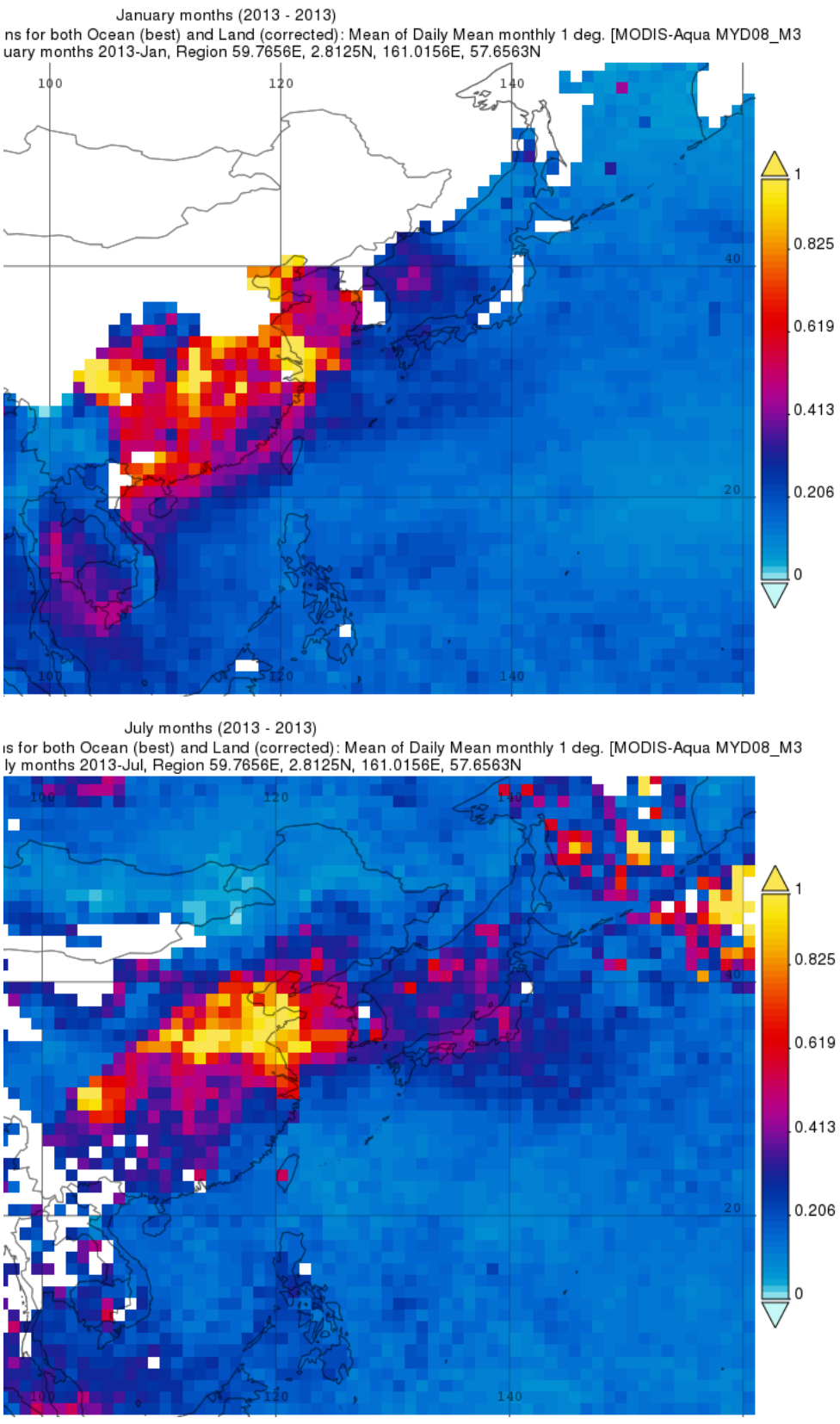

Figure S12. Monthly averaged AOD at 550nm observed by MODIS AQUA during January and July of 201301.

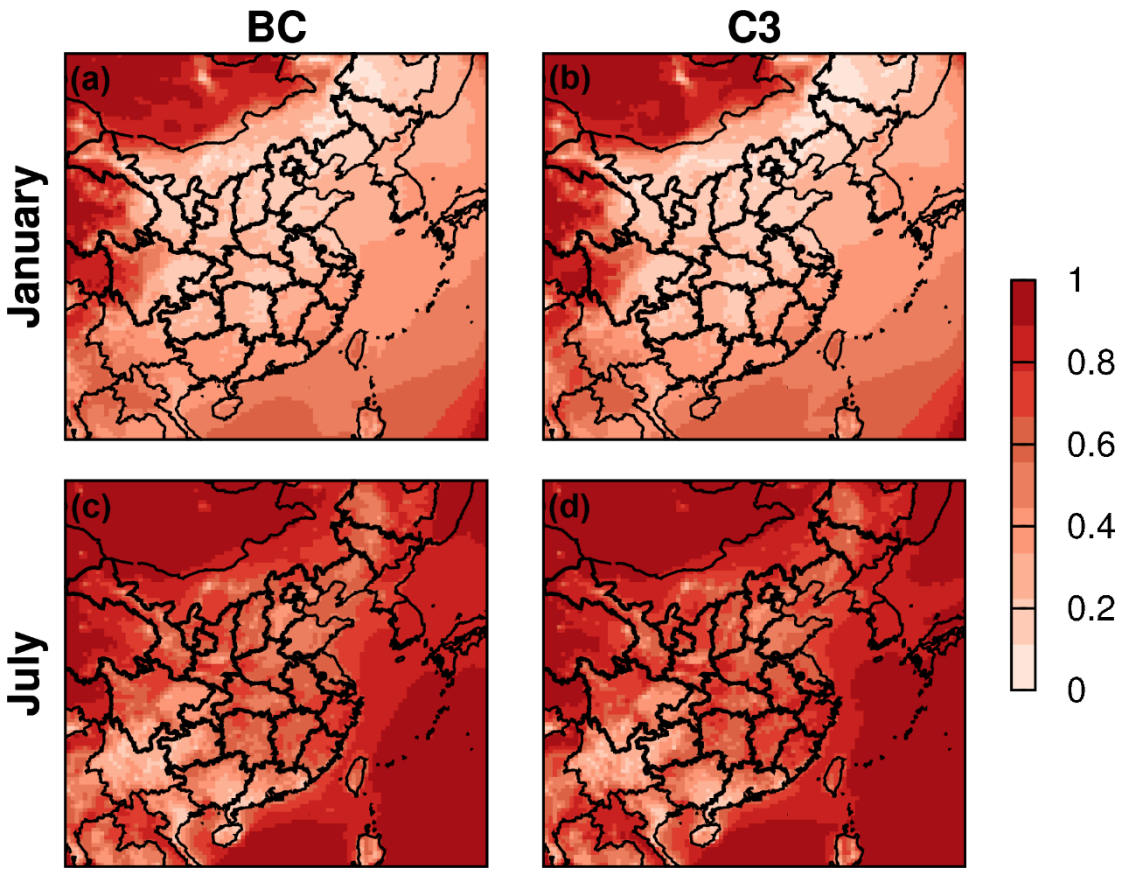

Figure S13. Averaged SOA/OA ratio from case BC and C3 during January and July of 2013.

References

Pankow, J. F., Marks, M. C., Barsanti, K. C., Mahmud, A., Asher, W. E., Li, J., Ying, Q., Jathar, S. H., and Kleeman, M. J.: Molecular view modeling of atmospheric organic particulate matter: Incorporating molecular structure and co-condensation of water, Atmos. Environ., 122, 400-408, https://doi.org/10.1016/j.atmosenv.2015.10.001, 2015.